Journal of
Nanoscience and Nanotechnology
Vol. 7, 1–9, 2007

Electrochemical Investigations of 3-(3-Thienyl) Acrylic Acid Protected Nanoclusters and Planar Gold Surfaces

R. G. Nirmal, A. L. Kavitha, Sheela Berchmans*, and V. Yegnaraman

Central Electrochemical Research Institute, Karaikudi 630006, Tamilnadu, India

Formation of self assembled monolayers on gold surface by thiols and disulphides is a well known phenomenon and extensive research work has been carried out in this area with envisaged applications in the area of sensors, molecular electronics, lithography, device fabrication using bottom-up approach, etc. Recently, it has been established that thiophene molecules can self assemble on gold surface due to Au–S interactions. 3-(3-thienyl) acrylic acid, a bifunctional ligand is used in this work to form self-assembled monolayers on planar gold surfaces (two dimensional assemblies) and to prepare monolayer protected gold nano clusters (three-dimensional assemblies). The electron transfer blocking properties of the two-dimensional monolayers were evaluated by using standard redox probes like ferrocyanide anions and Ruthenium hexamine cations. The functionalisation of the two-dimensional and three-dimensional assemblies has been carried out with ferrocene carboxylic acid and the functionalised monolayers were characterized by Cyclic voltammetry. The formation of thienyl acrylic acid protected nanoclusters has been verified by TEM and surface plasmon resonance absorption. It has been observed that when thiophene based ligands are used as stabilizers for the formation of metal nanoparticles, they tend to aggregate as a result of $\pi-\pi$ interactions between adjacent thiophene ligands. In this case it is found that aggregation is prevented. The substituent at the thiophene ring hinders $\pi-\pi$ interactions. The quantised nature of electrochemical charging of these nanoparticles has been demonstrated by differential pulse voltammetry (DPV), which exhibit peak like features (coulomb's staircase). This work also explores the possibility of using 3-(3-thienyl) acrylic acid as building blocks or spacers on planar and colloidal gold surfaces for potential applications in the field of sensors and devices.

Keywords:

RESEARCH ARTICLE

1. INTRODUCTION

Nanofabrication is the process of making functionalized structures with patterns having minimum dimensions up to 100 nm. Nanofabrication methodologies aided by nanomaterials will lead to newer technologies that will find exciting applications in the areas of information processing and storage, optics, materials science, catalysis, sensors, etc. Nanomaterials are mostly synthesized by either "top down" or "bottom up" approach. The latter approach exploits interactions between molecules or colloidal particles to assemble into discrete 2D and 3D nanoscale structures. The phenomenon of self assembly offers an easy and elegant route for the construction of organized 2D and 3D molecular assemblies on solid substrates.[1] Self assembled monolayers (SAM) on planar gold surfaces offer a vast scope for further functionalisation of the basic monolayers, which can be utilized for various applications. Also, SAM-stabilized metal nanoclusters serve as building blocks or nucleii for the construction of 3D molecular assemblies. Thus, SAMs act as scaffolds for constructing 3D and 2D assemblies. SAM based nanoarchitecture is akin to brick and mortar assemblies used in the construction of buildings.

SAM is formed through molecular organization caused by spontaneous adsorption of organic molecules on solid substrates such as Au and Si.[2–5] SAMs are usually fabricated by two different methods, vapor deposition in ultra high vacuum or immersion in a solution containing the monolayer-forming adsorbate. The SAM formation is influenced by adsorbate–substrate and adsorbate–adsorbate (eg., Van der Waals) interactions. Of all the SAMs, those of organosulphur compounds such as alkane thiols and thiophenes on Au, formed through Au–S interactions have received the greatest attention by researchers.

SAMs of thiophene compounds on Au is of special interest owing to their applications in electronic and

*Author to whom correspondence should be addressed.

optoelectronic devices.[6,7] Since the device characteristics are strongly determined by structural defects in the film and at the interfaces in contact, fabrication of high quality thiophene derivative films on substrates has been an important research goal.[8–14] Organosulphur compounds used for forming planar or 2D monolayers on metal substrates like Au can be utilized to stabilize metal nanoclusters by forming a 3D core around the metal nanoclusters. Monolayer protected nanoclusters (MPCs) are used as building blocks to fabricate 3D assemblies.

In this work, 3-(3-thienyl) acrylic acid, having a terminal carboxyl group is used for the formation of 2D or planar monolayers on Au substrates and also for stabilizing gold nanoclusters by forming a 3D shell. The carboxyl group enables building up of molecular assemblies over the monolayer. The 2D and 3D monolayers are characterized by electrochemical and spectral techniques. The electron transfer (ET) blocking properties of 2D monolayer, their functionalisation properties, the quantized nature of MPCs and their interaction with ferrocene carboxylic acid are discussed in this paper.

2. EXPERIMENTAL DETAILS

2.1. Chemicals

3-(3-Thienyl) acrylic acid (TAA), ferrocene carboxylic acid (FCA), ruthenium hexamine(III) chloride, and 1,1′-azobiscyclohexane carbonitrile (all from Aldrich), ethanol, potassium ferrocyanide, tetra *n*-octyl ammonium bromide, dichloromethane, methyl morpholine, dimethyl formamide (DMF), ethyl chloroformate, and $HAuCl_4$ (all from Merck), sodium borohydride (from SRL), were used as received.

2.2. Formation of TAA SAM on Planar Gold Substrates

SAMs on Au substrates were formed by immersion of the substrates (0.1 M) in an ethanol solution of TAA. After 24 h, the substrates were washed with ethanol, dried under N_2 and stored. The SAM layers were annealed by warming to 313 K with a 60 W incandescent lamp. The Au surfaces modified with 'as-formed' and 'annealed' TAA layers are denoted as 'Au/TAA' and 'Au/TAA-annealed' electrodes, respectively. After cooling to room temperature, the monolayers were characterized by IR and AFM. The TAA film was exposed to UV light in presence of 1,1′-azobiscyclohexane carbonitrile for 30 min to explore 2D polymerization on the monolayer. The resulting modified electrode is denoted as 'Au/TAA-UV' (Scheme 1). Voltammetric investigations were carried out to analyse the electron transfer blocking properties of the monolayer. Voltammograms were recorded using potentiostat (Wenking LB 75L) and voltage programmer (Wenking, VSG 72) coupled to a Rikadenki X-Y/t recorder. IR spectrum was recorded using grazing angle accessory (85°) with Nicolet 670 FT IR spectrophotometer.

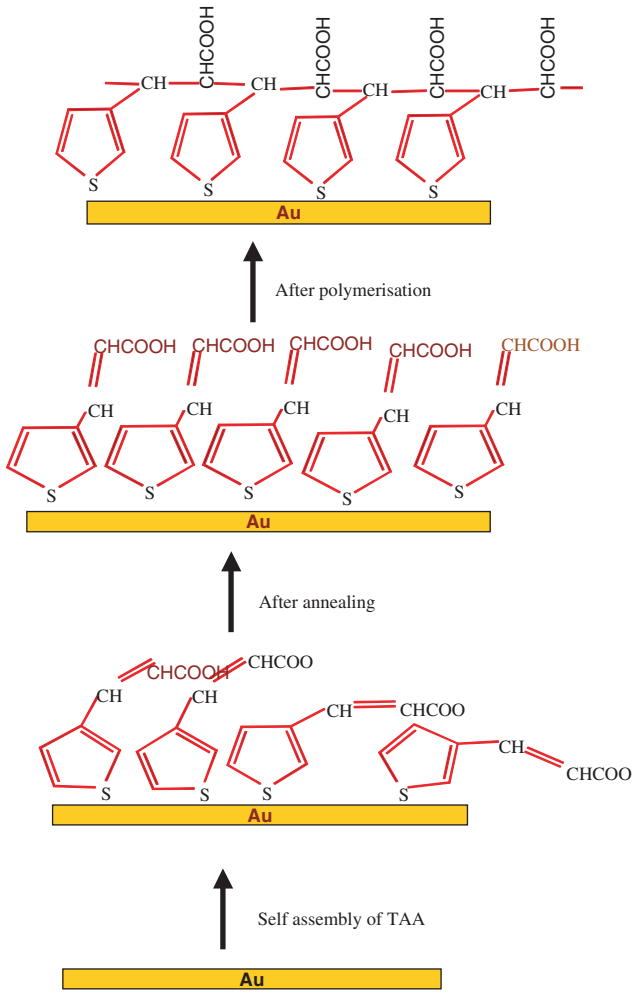

Scheme 1.

2.3. Functionalisation of Au/TAA with FCA

Au/TAA was treated with a solution containing methyl morpholine (20 μl) and ethyl chloroformate (20 μl) in DMF and kept in ice-cold condition for 15 minutes. Then it was washed in DMF and dipped in an ethanol solution of FCA (1 mM) for 30 minutes. The substrate was then washed with water, dried under nitrogen and stored. The carboxylic acid groups of TAA were activated by adding methyl morpholine. Methyl morpholine generates the carboxylate anion which then reacts with ethyl chloroformate to give mixed anhydride which then reacts with FCA.[15–17]

AFM images were recorded with the Molecular Imaging PicoSPM using gold-coated silicon nitride 30 nm cantilevers (force constant of 0.12 N/m). TEM was recorded using a Philips CM 200 tunneling electron microscope using a 400-mesh ultra thin carbon type A copper grid. UV spectrum was recorded using Varian Cary 50 spectrophotometer.

2.4. Preparation of TAA Protected Nanoclusters

For the synthesis of MPCs, the biphasic procedure developed by Brust et al.[15] was used. $HAuCl_4$ (0.8 mM) was transferred to the organic phase (toluene) using the phase transfer reagent tetra *n*-octyl ammonium bromide (0.6 mM). Then stabilizer, TAA was added to the organic phase. The solution was continuously stirred for two hours. Sodium borohydride (60 mM) was then added and it resulted in dark pink colour, which indicates the formation of gold nanoparticles. The solution was continuously stirred for eight hours and the gold nanoparticles were separated by rotary evaporation. The evaporated sample was treated three times with methanol to remove excess stabiliser and finally dried and stored for further use. The solution of nanoclusters was prepared by dissolving in dichloromethane.

DPV was recorded using PARSTAT 2263. The experimental parameters were as follows: pulse width 0.025 V for 50 ms, step height 2 mV, step time 100 ms, and scan rate 20 mV/s. For all electrochemical experiments a gold disc electrode of φ3 mm was used. Pt was used as the counter electrode and a Hg/Hg_2SO_4 was used as the reference electrode. For IR and AFM studies gold slides (1000 Å Au coating on Si wafers with an intermediate adhesion layer of 100 Å thick Ti, M/s Lance Goddard Associates, USA) of 1 cm × 1 cm size were used.

3. RESULTS AND DISCUSSION

Figure 1 presents the IR spectrum of solid TAA taken using KBr pellet. The characteristic absorption bands correspond to C═O stretch at 1675 cm^{-1} and C═C stretch at 1613 cm^{-1}. The ring stretch characteristic of thiophene ring occurs at 872 cm^{-1}. The out of plane deformation vibration of –C–H is observed at 654 cm^{-1}.

Figures 2(a–c) represents the IR spectra for the SAMs of TAA prepared under three different conditions described

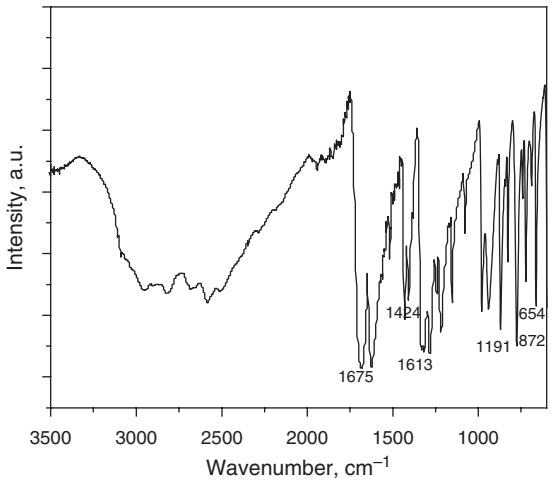

Fig. 1. FTIR spectrum for TAA-solid taken with KBr pellet.

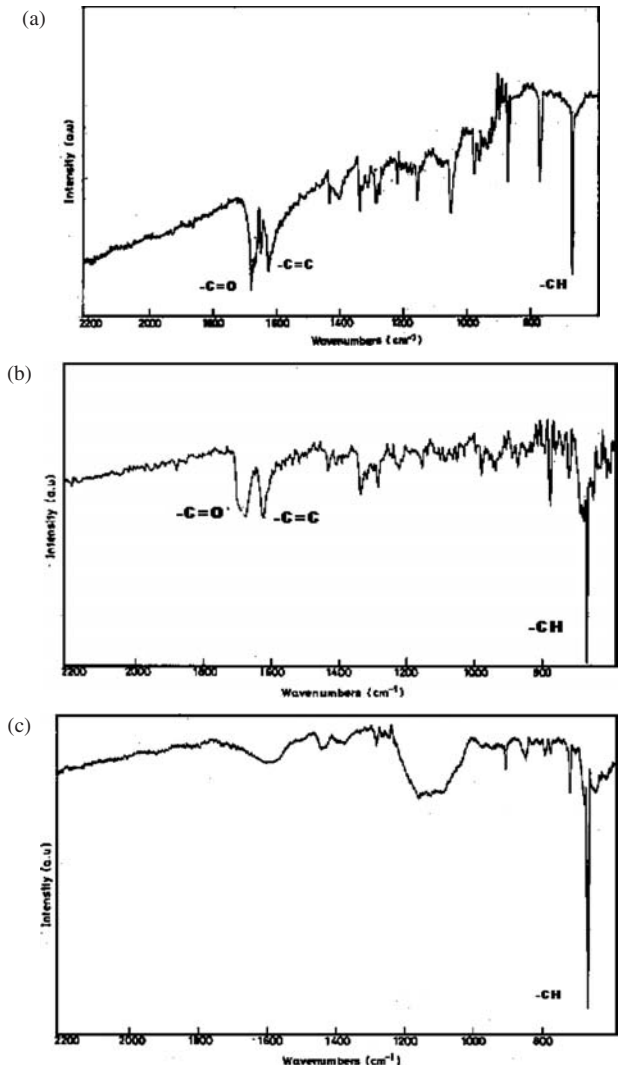

Fig. 2. FTIR-85° grazing angle spectra of TAA monolayer on (a) Au/TAA, (b) Au/TAA-annealed, and (c) AU/TAA-UV.

in the experimental section. The spectral changes were followed with the three principal bands corresponding to –C═O stretch, –C═C– stretch, and –C–H out of plane deformation stretch as marked in the figures. In Figure 2(b) the –C═O– and –C═C– stretch are well resolved compared to Figure 2(a). This shows the effect of annealing the Au/TAA films. However, the film exposed to UV light shows a dramatic change. The disappearance of C═C stretch and appearance of new CH_2 stretch at 2925 cm^{-1} (not shown in the figure) indicates 2D polymerization in presence of UV light indicating that the acrylic acid groups are polymerized on the substrate. Similar polymerization effect has been observed in the case of poly diacetylene monolayers on gold surfaces.[18] However polymerization did not disturb the gold-thiophene interactions as revealed by the intact C–H deformation stretch at 670 cm^{-1}. These bands are particularly very sharp in all the three cases indicating strong gold-thiophene interactions. The peak is sharper compared to that observed in the solid state.

RESEARCH ARTICLE

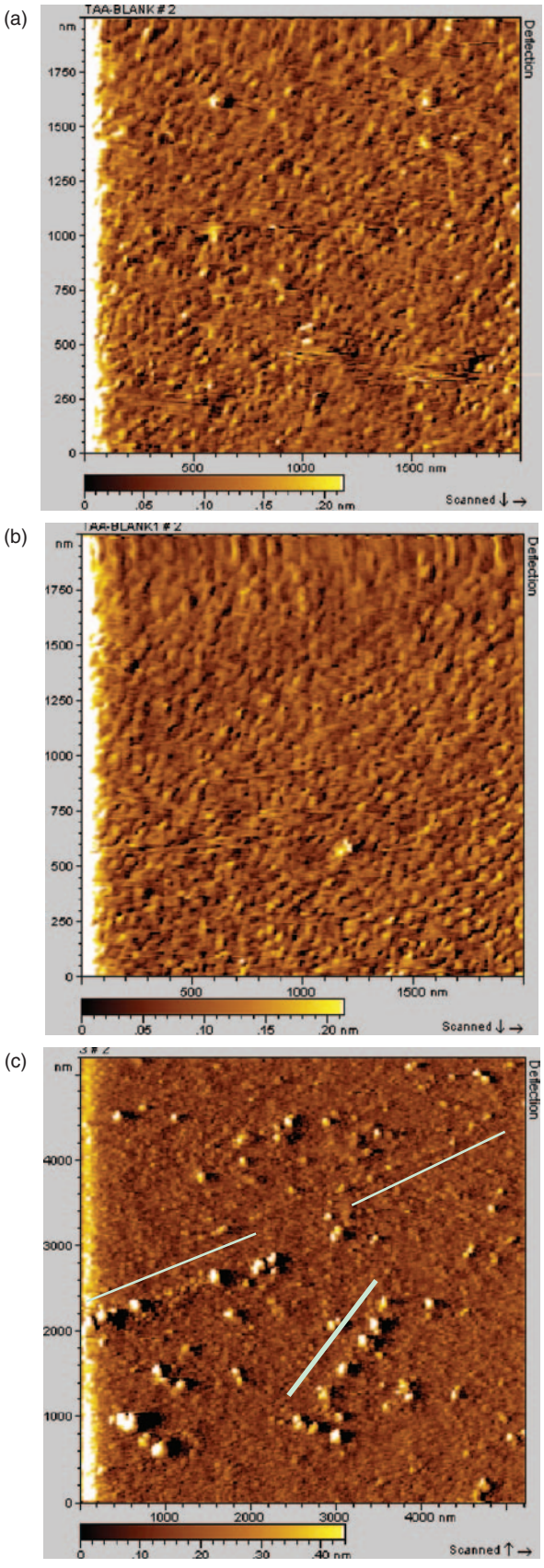

Fig. 3. AFM images of (a) AU/TAA, (b) AU/TAA-annealed, and (c) AU/TAA-UV.

Thiophene adsorption onto Au(111) raises some interesting questions about sulphur based monolayers because the sulphur atom in thiophene is a part of the stable aromatic ring. Unlike alkane thiols and dialkyl sulphides which can readily react with a gold surface, thiophene is relatively inert. It is difficult to reduce and its ring structure is difficult to cleave. In the case of dialkyl disulphides, which are prone to reductive S–S cleavage, the formation of surface thiolates takes place upon chemisorption. Similarly, chemisorption of alkane thiols leads to the formation of surface thiolates, but the fate of the hydrogen atoms from the thiol functional group is yet to be convincingly established. Unlike disulphides, which might be reductively cleaved and alkane thiols, which might be reduced to thiolates, the likelihood of thiophene participating in chemical reactions beyond simple molecular adsorption is quite small. Literature reports clearly demonstrate that the stages of thiophene growth process on gold surface undergo distinct phase structures. In the primary stage, thiophene assumes the parallel orientation with respect to the gold surface. Finally, thiophene switches over to an upright orientation in relation to the surface. The balance between the thiophene–gold and thiophene–thiophene interactions plays an important role in the SAM formation of thiophene.[10–14]

Figures 3(a–c) presents the AFM images of the three monolayers AU/TAA, AU/TAA-annealed, and AU/TAA-UV. The degree of organization of the film is seen to increase from 'a' to 'b' as seen by the decrease in white spots which represent in homogenities on the woven mat like surface of TAA monolayers. Figure 3(c) shows the 2D polymerization effect on the surface. After polymerization the monolayer looks more organized in a linear pattern. The green line represents the directional arrangement of the polymer film.

Figures 4(a–c) depicts the cyclic voltammograms (CV) representing the electron transfer (ET) blocking properties of the monolayer for ferro-/ferri-cyanide redox system 1 M H_2SO_4. CVs recorded under similar experimental conditions in 0.5 M Na_2SO_4 are given in Figures 5(a–c). In H_2SO_4 medium, compared to bare Au electrode, a marginal blocking is observed in the case of AU/TAA film while the polymerized film offers a significant barrier to ET. The current has significantly decreased compared to bare electrode and the ΔE_p has drastically increased to 280 mV. In Na_2SO_4 medium (Figs. 5(a–c)) Au/TAA film also shows appreciable barrier properties, which is reflected by the ferrocyanide peaks becoming broader and ΔE_p increasing to 260 mV. The currents have also decreased especially, the cathodic current. In the case of polymerized film, only irreversible electron transfer with decreased peak is observed. With $[Ru(NH_3)_6]^{3+}$ species, the voltammetric behaviour is similar to that of ferrocyanide. Only in the case of polymerized film (Figs. 6(a–c)), some electron transfer blocking is observed in H_2SO_4 medium. In Na_2SO_4 medium also, a similar effect is observed as shown in

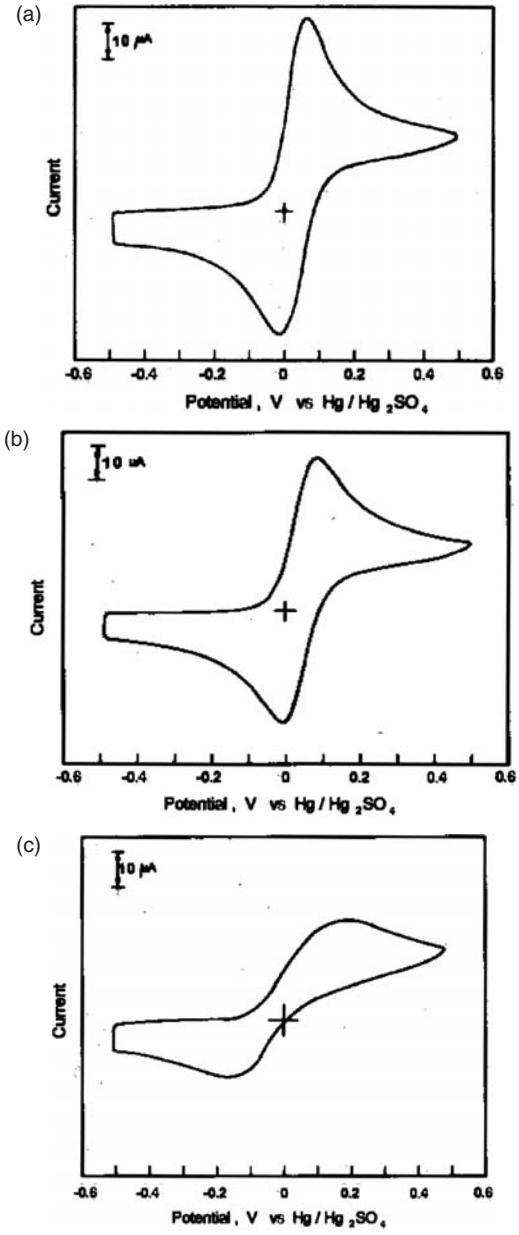

Fig. 4. Cyclic voltammogram for ferrocyanide electron transfer in 1 M H_2SO_4 at scan rate of 50 mV/s (a) bare Au, (b) Au/TAa, and (c) Au/TAA-UV.

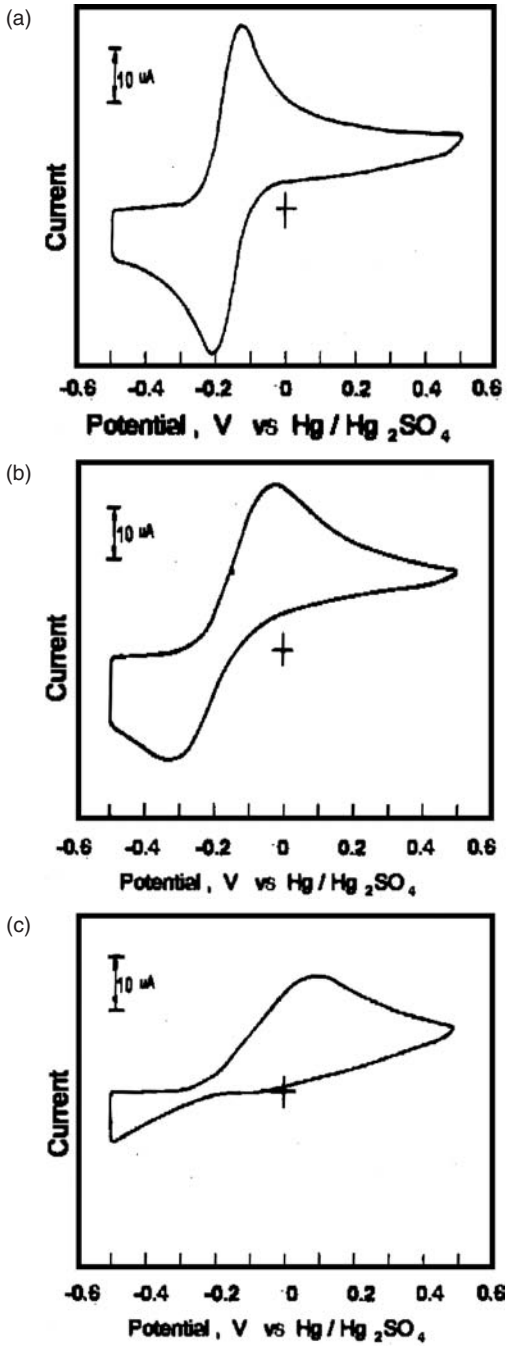

Fig. 5. Cyclic voltammograms representing ferrocyanide electron transfer in 0.5 M Na_2SO_4 at a scan rate of 50 mV/s (a) bare Au, (b) Au/TAA, and (c) Au/TAA-UV.

Figures 7(a–c). From the results observed, we can interpret the observations based on the IR spectral data information. Based on our results and literature reports, it is understood that there exists strong adsorption of thiophene on the substrates. Initially the rings are parallel to the substrate, which is followed by an upright position with respect to the plane of the substrate. The substituent–CH=CHCOOH is present in the 3-position. The electron transfer kinetics across a carboxylic terminated SAM layer is a function of three factors, viz., length of the carbon chain, structural organisation of the monolayer and electrostatic interactions between terminal functional groups and the probe molecules. In the case of TAA SAMs, we expect the negatively charged ferrocyanide ions to be blocked at neutral pH due to electrostatic repulsion between the ferrocyanide ions and the carboxylate terminal groups of SAMs. The influence of structural organisation is a measure of compactness of the monolayer which determines the pinholes and defects and can be predicted by the measurement of coverage. Since the electron transfer kinetics is a function of pH, the coverage estimation will not be reliable, as we will get different values at

RESEARCH ARTICLE

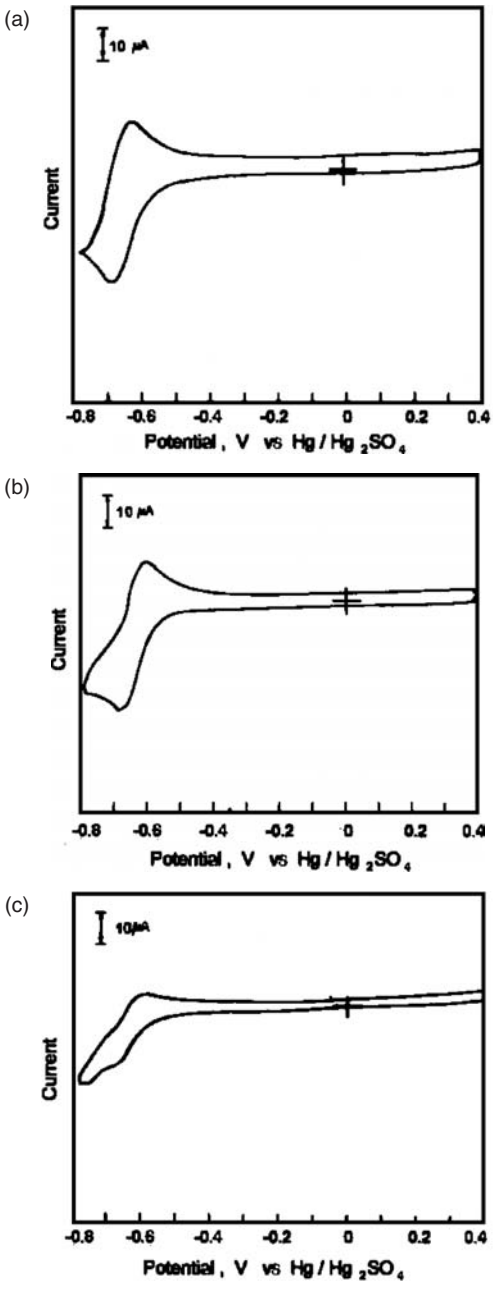

Fig. 6. Cyclic voltammograms representing $[Ru(NH_3)_6]^{3+}$ electron transfer in 1 M H_2SO_4 at a scan rate of 50 mV/s (a) bare Au, (b) Au/TAA, and (c) Au/TAA-UV.

coverage at different pH. Hence the observed behaviour is a combined effect of electrostatic interactions and structural organisation. One more factor which affects the electron transfer kinetics in this case will be the Π electron conjugation present in the ring and the substituent. This may improve the electron transfer kinetics at the SAM layer. Similar effect has been reported by us earlier.[19, 20] Hence ET is controlled both by ring, the substituent group and by structural organisation of the monolayer. In the case of polymerized films, the blocking observed is maximum as the polyacrylic acid groups formed on the surface

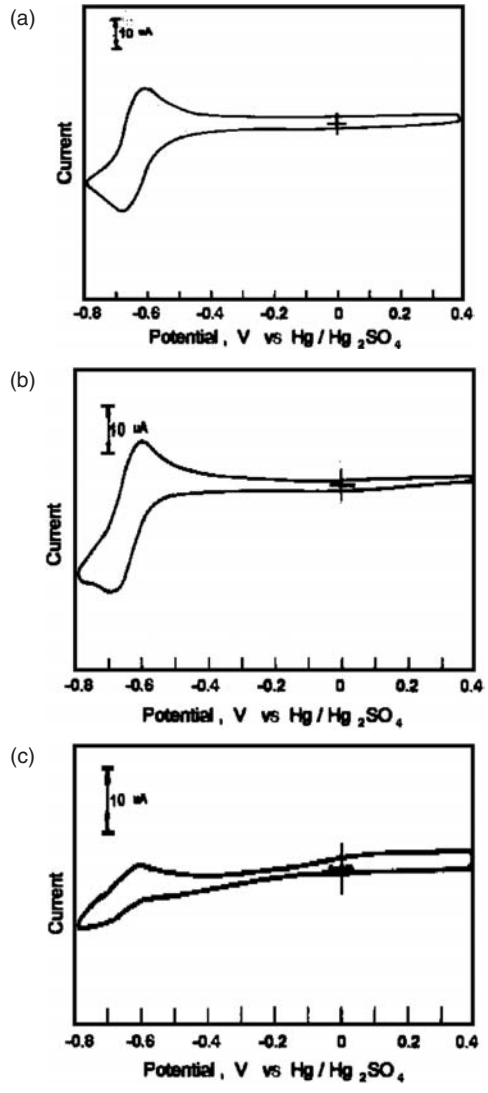

Fig. 7. Cyclic voltammograms representing $[Ru(NH_3)_6]^{3+}$ electron transfer in 0.5 M Na_2SO_4 at a scan rate of 50 mV/s (a) bare Au, (b) Au/TAA, and (c) Au/TAA-UV.

physically block the species from reaching the electrode surface to a greater extent than the –CH═CH–COOH groups on the surface.

Figure 8 shows the response of Au/TAA surface further modified with FCA in 1 M perchloric acid. A near reversible response is observed. A peak separation of nearly 80 mV is observed. The peak separation may arise due to the SAM layer, which impedes ET. This observation demonstrates the feasibility of building up 2D assemblies on SAM based platforms which can be used for different applications such as sensors, devices, etc.

Figure 9 presents the TEM images of gold nanoclusters stabilized by TAA. The TEM images reveal that the particles are nearly monodisperse and the average size of the particles lie in the range of 3–8 nm corresponding to a metal–ligand ratio of 1:6. The particles are arranged in such a way that a hexagonal arrangement of particles

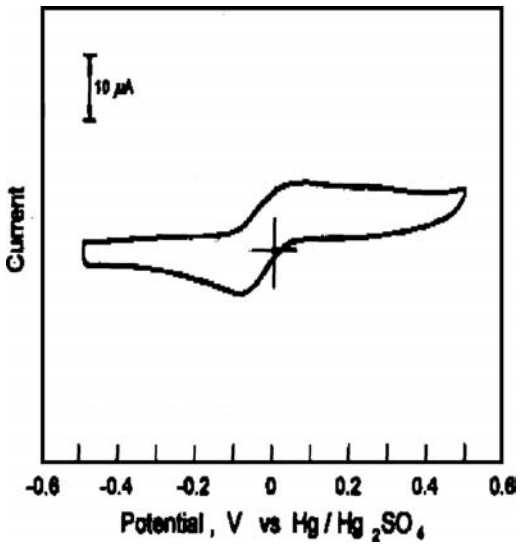

Fig. 8. Cyclic voltammogram representing the functionalisation of Au/TAA monolayer with FCA in 1 M perchloric acid at a scan rate of 50 mV/s.

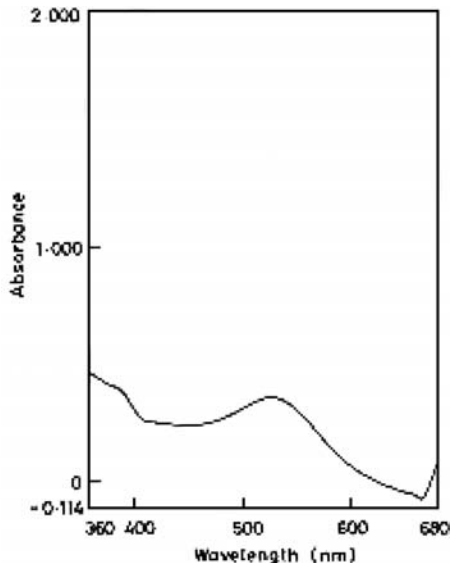

Fig. 10. UV spectrum of TAA stabilized gold nanoclusters.

can be seen from the TEM image. An array like arrangement of particles is also seen. The size distribution curve is given in Figure 9(b). The major size distribution lies around 5 nm. A higher ratio of ligand to metal decreases the particle size and 2–3 nm particles can be prepared with a ligand to metal ratio of 10:1.

Figure 10 depicts the UV spectrum of the nanoclusters dissolved in dichloromethane. The maximum appears at 515 nm, which corresponds to the surface plasmon resonance reported in the literature. A small peak seen in the lower wavelength side corresponds to that of the ligand.

Figure 11 represents the DPV of nanoclusters dissolved in the electrolyte 0.1 M tetrabutyl ammonium tetrafluoborate in dichloromethane. The peak like features seen in DPV correspond to that of coulomb staircase charging events. Each successive current peak corresponds to a single electron charging of MPCs, that diffuse to the electrode surface. The formal potentials for successive quantized double layer capacitance charging, $z/z-1$ can be shown

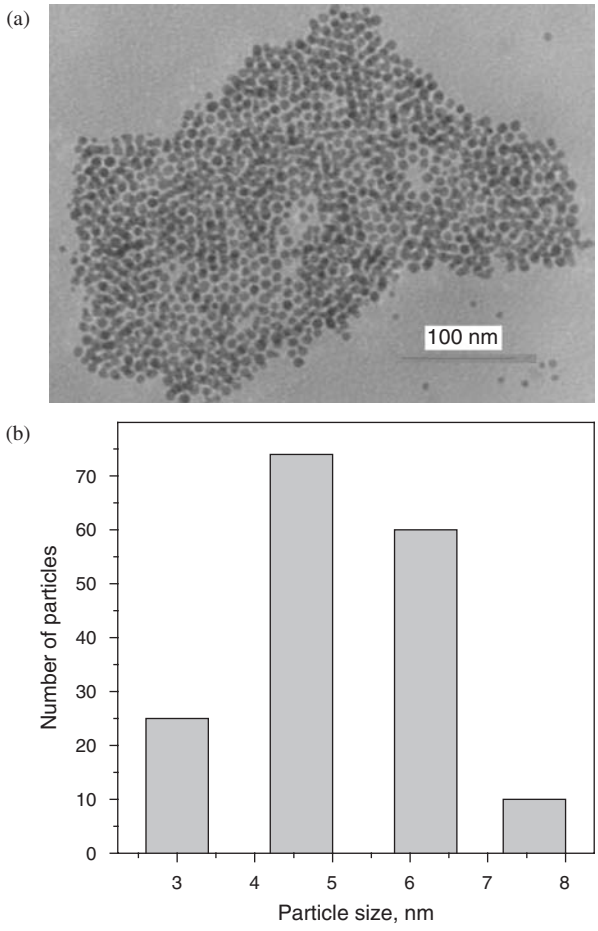

Fig. 9. (a) TEM image of TAA protected gold nanoclusters, (b) size distribution curve.

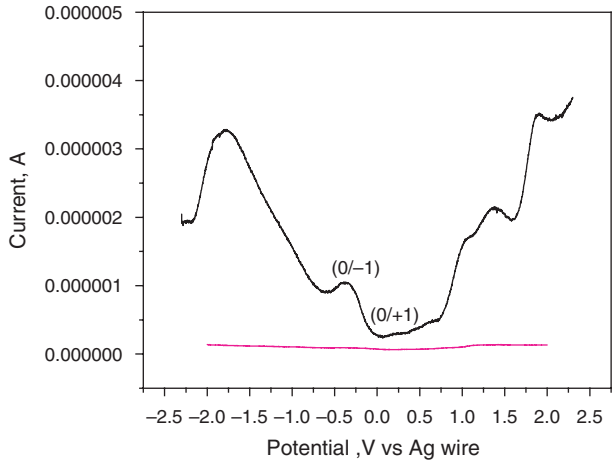

Fig. 11. DPV showing the quantized nature of TAA protected gold nanoclusters: Pink line refers to the background.

RESEARCH ARTICLE

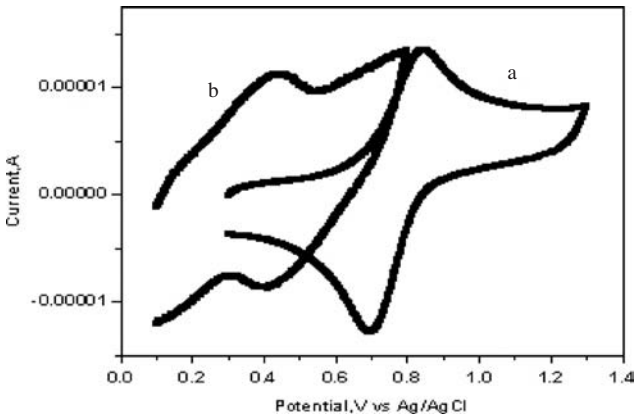

Fig. 12. CVs representing (a) reversible ET for FCA (1 mM) on and (b) interactions of Au-TAA nanoclusters (1 mg) with FCA on gold electrode. Supporting electrolyte: tetrabutyl ammonium tetrafluoborate (0.1 M), Solvent: dichloromethane, Scan rate 50 mV/s.

to vary with charge state as

$$E^0_{z/z-1} = E_{\text{pzc}} + (z - 1/2)e/C_{\text{cluster}} \quad (1)$$

where E_{pzc} is the potential of zero charge ($z = 0$) corresponding to the nanoclusters.

The potential of zero charge (PZC) can be estimated from the double layer capacitance variation with potential. Double layer capacitance is well known to exhibit a minimum near PZC of an electrified interface. Equation (1) predicts a linear plot of charging peak potentials against charge state. The charge state $z = 0/+1$ is for example assigned to the first DPV peak that is positive to E_{pzc}.[21–23] The PZC was estimated to be –0.2 V. The peaks corresponding to $0/+1$ and $0/-1$ are marked in the figure Δv corresponding to these two peaks is found to be 0.57. The charging properties of the clusters are classified as molecule like or metal like depending on the value of Δv.[24–26] Laege Δv values correspond to molecule like charging. The Δv value observed by us is in between molecule like and metal like charging. Usually symmetrical peaks are observed for single electron transfer events. However in our case the peaks are not symmetrical. The reason is attributed to the capping ligands TAA. The Π conjugation present in the thiophene ring as well as in the acrylic acid substituent may have its influence on charging events which will be addressed in our future work.

Figure 12(a) represents the CV of FCA in dichloromethane +0.1 M tetrabutyl ammonium tetrafluoborate. A reversible feature is observed in this case. Figure 12(b) shows the CV of FCA hydrogen bonded to TAA-stabilized nanoclusters. The voltammogram shows irreversible features. This shows that the linking process slows down ET kinetics. It is known that ferrocene molecules incorporated on long chain SAM molecules exhibit reversible ET kinetics. Therefore better linking strategies need to be developed in this case to provide better ET kinetics.

Only a few reports are available where thiophene based ligands have been used as a stabilizer for the preparation of gold nanoclusters.[27–31] The nanoparticles stabilized by thiophene are found to undergo aggregation as a result of $\pi-\pi$ interactions between the rings. In our case, the nanoparticles remain stable for several weeks without aggregation. The substitution present in the 3-position prevents $\pi-\pi$ interactions and hence aggregation is not observed. The absence of aggregation can be seen clearly from UV data. Usually aggregation causes the coupling of the plasmon modes of the gold nanoparticles, which results in the red shift of the surface plasmon resonance in the UV spectrum. According to Mie scattering theory, which is often employed in explaining such red shifts, the theory predicts that shifts in the surface plasmon resonance can occur when the particles deviate from spherical geometry such as in aggregates. Under these circumstances, the transverse and longitudinal dipole polarisability no longer produces equal resonances. Consequently, two plasmon resonances appear: a broad and red shifted longitudinal plasmon resonance and a transverse plasmon resonance. Our results reveal the presence of single plasmon resonance centred at 515 nm. This suggests clearly that no aggregation is present in this case. This is an added advantage when these nanoclusters are used as building blocks for the construction of 3D assemblies.

4. CONCLUSIONS

In this work, formation of 2D monolayers of 3-(3-thienyl) acrylic acid on planar gold substrates, the formation of 3-(3-thienyl) acrylic acid stabilised gold nanoclusters and their functionalisation by ferrocene carboxylic acid is described. The 2D monolayers on gold surface were characterized by FTIR spectral data. The ET blocking properties were studied using ferrocyanide anions and ruthenium hexamine cations. The functionalisation of monolayers with ferrocene carboxylic acid is demonstrated.

The 3D monolayers of TAA on gold nanoclusters prevent aggregation of gold nanoparticles by preventing $\pi-\pi$ interactions between thiophene rings due to the presence of acrylic acid as a substituent in the 3-position. The nanoclusters were characterized by TEM and UV measurements. The quantized nature of charging is demonstrated by DPV experiments. The interaction between ferrocene carboxylic acid and the gold nanoclusters indicates the scope for building 3D molecular assemblies around the nanoclusters.

Acknowledgment: The authors thank Department of Defence Research and Development Organization, New Delhi for financial support.

References and Notes

1. R. Shenhar and V. M. Rotello, *Acc. Chem. Res.* 36, 549 (**2003**).
2. R. G. Nuzzo and D. L. Allara, *J. Am. Chem. Soc.* 105, 4481 (**1983**).
3. M. R. Linford and C. E. D. Chidsey, *J. Am. Chem. Soc.* 115, 12631 (**1993**).

4. A. Ulman, An Introduction to Ultra Thin Organic Films from Langmuir-Blodgett to Self Assembly, Academic Press, San Diego **(1991)**.
5. A. Ulman, *Chem. Rev.* 96, 1533 **(1996)**.
6. H. Sirringhaus, N. Tessler, and R. H. Friend, *Science* 280, 1741 **(1998)**.
7. L. Dodabalapur, L. Torsi, and E. Katz, *Science* 268, 270 **(1995)**.
8. J. Noh, K. Kobayashi, H. Lee, and M. Hara, *Chem. Lett.* 630, 2000 **(2000)**.
9. O. Onodera, T. Matsuura, T. Takamura, and Y. Shinoyama, *J. Surf. Sci. Soc. Jpn.* 20, 553 **(1999)**.
10. T. Matsuura and T. Shimoyama, *Eur. Phys. J. E* 7, 233 **(2002)**.
11. T. Matsuura, M. Nakajima, and Y. Shimoyama, *Jpn. J. Appl. Phys.* 40, 6945 **(2001)**.
12. M. H. Dishner, P. Taborek, J. C. Hemmenger, and F. J. Feher, *Langmuir* 14, 6676 **(1998)**.
13. R. Stecher, F. Drewnick, and B. Gompf, *Langmuir* 15, 6490 **(1999)**.
14. M. H. Dishner, J. C. Hemmenger, and F. J. Feher, *Langmuir* 12, 6176 **(1996)**.
15. R. O. C. Norman, Principles of Organic Synthesis, Wilmer Brothers Limited **(1968)**, p. 340.
16. M. L. Bruening, Y. Zhou, G. Aguilar, R. Agee, D. E. Bergbreiter, and R. M. Crooks, *Langmuir* 13, 770 **(1997)**.
17. T. Mary Vergheese and Sheela Berchmans, Electrochimica Acta, in press.
18. Sheela Berchmans, S. Arivukkodi, and V. Yegnaraman, *Electrochem. Commun.* 2, 226 **(2000)**.
19. Sheela Berchmans, V. Yegnaraman, and G. Prabhakara Rao, *Proc. Indian Acad. Sci.* (*Chem. Sci.*) 109, 277 **(1997)**.
20. N. K. Chaki, P. Singh, C. V. Dharmadhikari, and K. P. Vijayamohanan, *Langmuir* 20, 10208 **(2004)**.
21. S. Chen, R. W. Murray, and S. W. Feldberg, *J. Phys. Chem. B* 102, 9898 **(1998)**.
22. S. Chen and J. M. Sommers, *J. Phys. Chem. B* 105, 8816 **(2001)**.
23. M. Brust, M. Walker, D. Bethell, D. J. Schiffrin, and R. Whyman, *J. Chem. Soc. Chem. Commun.* 801 **(1994)**.
24. J. F. Hicks, D. T. Miles, and R. W. Murray, *J. Am. Chem. Soc.* 124, 13322 **(2002)**.
25. S. Chen, *J. Phys. Chem. B* 104, 663 **(2000)**.
26. S. Chen and R. W. Murray, *J. Phys. Chem. B* 103, 9996 **(1999)**.
27. J. Noh, E. Ito, K. Nakajima, J. Kim, H. Lee, and M. Hara, *J. Phys. Chem. B* 106, 7139 **(2002)**.
28. H. Ahn, M. Kim, D. J. Sandman, and J. E. Whetten, *Langmuir* 19, 5303 **(2003)**.
29. J. H. Youk, J. Locklin, C. Xia, M. A. Park, and R. Advincula, *Langmuir* 17, 4681 **(2001)**.
30. J. J. Storhoff, R. Elghanian, R. C. Mucic, C. A. Mirkin, and R. L. Letsinger, *J. Am. Chem. Soc.* 120, 1959 **(1998)**.
31. D. Patton, J. Locklin, M. Meredith, Y. Xin, and R. Advincula, *Chem. Mater.* 16, 5063 **(2004)**.

Received: Xx Xxxx Xxxx. Revised/Accepted: Xx Xxxx Xxxx.